Dalton Transactions

Accepted Manuscript

ROYAL SOCIETY OF CHEMISTRY

www.rsc.org/dalton

Osmium(II) Polypyridyl Polyarginine Conjugate as a Probe for Live Cell Imaging; A Comparison of Uptake, Localization and Cytotoxicity with its Ruthenium(II) Analogue.

Aisling Byrne,[†] Ciarán Dolan,[†] Roisin D. Moriarty,[†] Aaron Martin[†], Ute Neugebauer,[†] Robert J. Forster[†] Anthony Davies[b] Yuri Volkov[b] and Tia E. Keyes.[†]*

[†] School of Chemical Sciences, National Centre for Sensor Research, Dublin City University, Glasnevin, Dublin 9, Ireland.

[b] School of Medicine, CRANN and AMBER Centres, Trinity College Dublin, Dublin 2, Ireland

* *Corresponding authors: tia.keyes@dcu.ie*

KEYWORDS. Osmium, Ruthenium, Octa-arginine peptide, Cell uptake high throughput (HTP) studies

Supporting Information Placeholder

ABSTRACT: A first investigation into the application of a luminescent osmium(II) bipyridine complex to live cell imaging is presented. Osmium(II) (bis-2,2-bipyridyl)-2(4-carboxylphenyl) imidazo[4,5f][1,10]phenanthroline was prepared and conjugated to octaarginine, a cell penetrating peptide. The photophysics, cell uptake and cytotoxicity of this osmium complex conjugate were performed and compared with its ruthenium analogue. Cell uptake and distribution of both ruthenium and osmium conjugates were very similar with rapid transmembrane transport of the osmium probe (complete within approx. 20 mins) and dispersion throughout the cytoplasm and organelles. The near-infrared (NIR) emission of the osmium complex (λ_{max} 726 nm) coincides well with the biological optical window and this facilitated luminescent and luminescence lifetime imaging of the cell which was well resolved from cell autofluorescence. The large Stokes shift of the emission also permitted resonance Raman mapping of the dye within CHO cells. Rather surprisingly, the osmium conjugate exhibited very low cytotoxicity when incubated both in the dark and under visible irradiation. This was attributed to the remarkable stability of this complex which was reflected by the complete absence of photo-bleaching of the complex even under extended continuous irradiation. In addition, when compared to its ruthenium analogue its luminescence was short-lived in water therefore rendering it insensitive to O_2.

Introduction

The last 8 years have seen something of a paradigm shift in the development of probes for optical bioimaging as luminescent complexes of the d-block elements are being increasingly validated as alternatives to conventional organic fluorophores.[1,2] Their advantages are myriad, including tuneable emission, photostability and Stokes shifted emissions.[3,4,5,6,7] Through modification/bioconjugation such metal complexes have been rendered water soluble and cell permeable and increasingly, means of more focussed targeting within the cell is emerging.[8,9,10,11,12,13,14,15,16]

Thus far, most of the focus has been on ruthenium, rhodium and iridium polypyridyl complexes. Interest in these metals, particularly in ruthenium, has been built on the extensive insights generated on their interactions with biopolymers, particularly DNA, over the past three decades.[17,18,19,20,21,22,23,24]

Whilst osmium complexes featuring labile ligands have been the focus of numerous important studies as anti-cancer agents, osmium polypyridyl complexes have not, to our knowledge, been examined to date in the context of their capacity as cellular imaging probes [25,26,27,28,29] Osmium(II) polypyridyl complexes share many of the photophysical advantages of their ruthenium(II) analogues. Although their emission quantum yields and lifetimes tend to be lower, they have two key additional benefits; firstly, osmium(II) polypyridyl complexes typically exhibit emission maxima in the NIR spectral region below 700 nm, i.e. strongly coincident with the biological optical window. Secondly, because of their increased crystal field splitting, the osmium d-d states cannot be accessed by thermal cross-over from its excited triplet state, as is the case for ruthenium.[30,31] Therefore, osmium(II) polypyridyl complexes tend to exhibit relatively temperature independent photophysics and exceptional photostability.[32,33] This is an important concern in cell imaging where in most instances cells are incubated at 37°C during imaging. For many ruthenium polypyridyl complexes increased temperature can lead to significant reductions in emission intensity and lifetime[34] and reduced photostability of the complex due to thermal population of the e_g* state from the triplet excited state in these complexes.[30,35,36] This is particularly true in aqueous

solutions and media containing anions such as Cl^-, (e.g. the saline environment used for cell imaging) where the chloro or aquo product can form from ligand loss.[30]

We previously described the cell permeability of a ruthenium polypyridyl complex; $[Ru(bpy)_2(picR_8)]^{10+}$ where bpy is 2,2-bipyridyl and picR8 is 2(4-carboxylphenyl) imidazo[4,5f][1,10]phenanthroline conjugated to an octa-arginine peptide in SP2 Myeloma cells. The peptide rendered the complex water soluble and cell permeable in aqueous media without requirement for permeabilization, for example with DMSO. At room temperature it was found that the complex exhibited good photostability and strong ^{3}MLCT emission which could be used to image the cell.

Herein, to understand if osmium polypyridyl complexes can be similarly directed across the cell membrane and to establish their suitability for cell imaging, we prepared the osmium(II) analogue and examined and compared the photophysics, cell uptake, distribution and cytotoxicity of both $[Ru(bpy)_2(picR_8)]^{10+}$ and $[Os(bpy)_2(picR_8)]^{10+}$. We found that uptake and localization within the cell were similar for each conjugate and notably that both complexes exhibited the same low cytotoxicity. However, although the osmium complex exhibited a weaker emission than ruthenium, it demonstrated remarkable photostability with emission in the NIR window making such complexes potentially useful in tissue imaging.

Materials and Methods

Materials

All chemicals and reagents were purchased from Sigma Aldrich (Ireland) and were used without purification unless otherwise stated. Cell culture media, serum, and penicillin/streptomycin were also acquired from Sigma Aldrich. Co-localising dyes were purchased from Life Sciences, and Resazurin agent from PromoKine. The NH_2-Ahx-R_8-$CONH_2$ (arg_8) peptide was purchased from CeltekPeptides, Franklin, USA.

Instrumentation

^{1}H NMR spectroscopy was performed on a Brucker AC 400 MHz. All NMR spectra were processed and analysed using Topspin NMR software. Thin layer chromatography (TLC) was performed on glass silica gel (Merck, 250 µm thickness) or C18 (Sorbent Technologies, 250 µm thickness) plates. High performance liquid chromatography (HPLC) was performed using a Varian LC 940 series with a Hichrom C18 250 x 4.6 mm column along with photodiode array detector (150-900 nm), a 50 µl injection loop, auto sampler and auto collector. Dual detection wavelength was set for 220 nm and 480 nm. The mobile phase was of HPLC grade quality, filtered and purged with nitrogen prior to use. Mobile phase A consisted of deionised water (with 0.1% v/v trifluoroacetic acid (TFA)) and mobile phase B contained acetonitrile (with 0.1% v/v TFA). The mobile phase gradient was initially set for 5%:95% (solvent A:solvent B) and ended up as a 50%:50% (solvent A:solvent B) mixture over the 45 min run time. Samples were also filtered (0.8 µm pore size) prior to injection. Electron spray ionisation (ESI) mass spectrometry experiments were carried out using a Micromass/Waters Corporation (USA) spectrometer with positive ion polarity ESI. Samples were dissolved in HPLC grade acetonitrile and were analysed by technicians at University College Dublin. MALDI-ToF mass spectrometry was performed on MALDI-Q-ToF Premier instrument at Trinity College Dublin. Trans-2-[3-(4-tert-butylphenyl)-2-methyl-2-propenylidene]malononitrile (DCTB) was used as the MALDI matrix. Elemental analysis was carried out on an Exador analytical CE440 analyser at the Microanalytical Laboratory in University College Dublin. UV-Vis spectra were recorded on a Jasco spectrophotometer. Results were recorded in a quartz cuvette with a pathlength of 1 cm with a spectral range of 200-900 nm. The background was corrected for blank solvent absorbance prior to measurement. Emission spectra were recorded on a Varian Cary Eclipse fluorescence spectrophotometer with excitation and emission slit widths of 10 nm. The background was corrected for blank fluorescence and all measurements were performed at room temperature, 294K. Luminescent lifetimes were obtained using time correlated single photon counting (TCSPC) PicoQuant system. The exciting laser was 450nm. 10,000 counts were collected for each lifetime measurement, and were performed in triplicate. Lifetimes decays were analysed using PicoQuant NanoHarp software.

Synthesis of Osmium(II) (bis-2,2-bipyridyl)-2(4-carboxylphenyl) imidazo[4,5f][1,10]phenanthroline, $[Os(bpy)_2(pic)]^{2+}.(ClO_4)^-_2$

2-(4-Carboxyphenyl)imidazo[4,5-f][1,10]phenanthroline (pic) was synthesized as reported previously.[37] ^{1}H NMR (400 MHz, DMSO-d_6): δ (ppm): **13.96** (s, 1H), **13.09** (s-broad, 1H), **9.05** (d, 2H), **8.95** (d, 2H), **8.40** (d, 2H), **8.17** (d, 2H), **7.87** (m, 2H).

Osmium-bis(2,2-bipyridyl)dichloride, $[Os(bpy)_2Cl_2]$, was prepared according to a procedure modified from the literature.[38] $OsCl_3.H_2O$ (500 mg, 1.69 mmol), 2,2'-bipyridine (527 mg, 3.37 mmol) and lithium chloride (913 mg, 21.5 mmol) were dissolved in N_2 purged DMF (25 mL) in a round bottomed flask. The reaction was then left refluxing at 180°C for 3 h under a nitrogen environment. The reaction was cooled to room temperature and triethylamine (960 µL, 6.89 mmol) was added and refluxed for a further 1.5 h under a nitrogen environment. The reaction was cooled to room temperature and an excess of acetone (150 mL) was added and kept in the freezer overnight to induce precipitation. The precipitate was collected and washed with thoroughly with acetone to yield the purple-brown

product (596 mg, 62%). ^{1}H NMR (400 MHz, DMSO-d_6): **δ** (ppm): **9.64** (d, 2H), **8.55** (dd, 2H), **8.35** (dd, 2H), **7.55** (m, 4H), **7.27** (t, 4H,), **6.77** (td, 2H).

$[Os(bpy)_2Cl_2]$ (100 mg, 0.174 mmol), pic ligand (71 mg, 0.209 mmol) were dissolved in N_2 purged ethylene glycol (15 mL) in a round bottomed flask. The reaction mixture was then left refluxing at 215°C for 18 h under a nitrogen environment. The reaction was cooled to room temperature and the crude product was precipitated using a saturated solution of lithium perchlorate. The precipitate was collected by vacuum filtration and washed thoroughly with water, diethyl ether and drier under vacuum. The product was purified by silica gel chromatography using 10% MeOH/CH_2Cl_2 as mobile phase to yield a dark green colored product (144 mg, 79%). ^{1}H NMR (400 MHz, DMSO-d_6): **δ** (ppm): **14.59** (s, 1H), **8.87** (m, 6H), **8.83** (d, 2H), **8.27** (dd, 2H), **8.00** (td, 4H), **7.89** (m, 4H), **7.74** (dd, 2H), **7.48** (td, 4H), **7.21** (t, 2H). *m/z* (ESI+) calc. for $C_{40}H_{27}N_8Na_2O_2Os$ $[M^+{+}2Na{-}H]^+$ 887.9039, found 887.2274. Elemental Analysis: Calculated (%) for $C_{40}H_{28}N_8O_{10}OsCl_2.2.5CH_2Cl_2$– C; 40.70, H; 2.65, N; 8.93. Found (%) C; 40.93, H; 2.66, N; 8.50. The purified complex showed a single peak on HPLC with retention time of 11.79 min.

Synthesis of $[Os(bpy)_2(pic\text{-}arg8)]^{10+}$

$[Os(bpy)_2(pic)]^{2+}.(ClO_4^-)_2$ (20 mg, 0.02 mmol) was added to HATU (19 mg, 0.051 mmol) in DMF (0.5 ml) and stirred for 20 min. DIPEA (14.8 µL, 0.085 mmol) was then added to the flask along with NH_2-Ahx-R_8-$CONH_2$ (23.5 mg, 0.017 mmol) in DMF (1.0 ml) and the reaction was allowed to stir at r.t for 16 h. A saturated KPF_6 solution was then added to the reaction mixture to induce precipitation of the product which was filtered and re-dissolved in EtOH:H_2O (1:1) and concentrated to a minimal volume and then re-precipitated and filtered to yield the dark green product (18 mg, 44%). ^{1}H NMR (400 MHz, $(CD_3)_2CO$-d_6): **δ** (ppm): **13.60** (s, 1H), **8.99** (s, 2H), **8.85** (m, 4H), **8.79** (m, 4H), **8.45** (d, 4H), **8.31** (m, 8H), **8.28** (m, 8H), **8.09-7.90** (m, 12H), **7.85** (dd, 2H), **7.75** (dd, 2H), **7.54** (dt, 4H), **7.28** (dt, 4H), **4.44** (m, 4H), **4.20** (m, 4H), **2.85** (m, 16H), **2.35-1.67** (m, 6H), **1.49-1.28** (m, 20H), **0.97-0.81** (m, 16H). MALDI-ToF calculated for $[Os(bpy)_2(pic\text{-}arg8)]^{10+}$ (m/z) 2214, found (m/z) 2209 ($[Os(bpy)_2(pic\text{-}arg8)]^{5+}$). The purified conjugate showed a single peak on HPLC with retention time of 10.04 min.

Photophysics and Stability of $[Os(bpy)_2(pic)]^{2+}$ and $[Os(bpy)_2(pic\text{-}arg8)]^{10+}$

Working stock solutions of the osmium(II) and ruthenium(II) parent complexes were prepared by dissolution in in PBS (containing 1% v/v DMSO) with sonication for 40 minutes and the solutions were stored in the freezer. The peptide conjugates; $[Os(bpy)_2(pic\text{-}arg8)]^{10+}$ and $[Ru(bpy)_2(pic\text{-}arg8)]^{10+}$ were readily soluble in PBS, without the need for DMSO as co-solvent.

To de-aerate the solutions, they were purged with nitrogen gas for 20 minutes and in O_2 dependent measurements the sample was allowed to re-aerate over time. The O_2 concentration in the sample was measured using a PreSense Oxygen Probe. The emission spectrum and lifetimes of the dye were measured at 230, 155, 75, and 0.5 µmol/L of oxygen, where 230 µmol/L corresponds to O_2 saturation of the sample and 0.5 µmol/L was the lowest O_2 concentration achieved in aqueous buffer after N_2 gas purging.

Cell Culture

Two cell lines were studied; Chinese hamster ovarian (CHO-K1), an adherent cell line and a murine myeloma spleen suspension cell line, SP2/0-Ag 14. The media used to culture the cells was Dulbecco's modified Eagle's medium (DMEM)/Hams F-12 for CHO and DMEM for SP2. Both were supplemented with 10% foetal bovine serum and 1% penicillin and streptomycin and grown at 37°C with 5% CO_2. Cells were harvested or split at 90% confluency for CHO (using 0.25% trypsin for 5 min at 37°C) and $1x10^6$ cells per mL for SP2 cells.

Confocal Microscopy

CHO and SP2 cells were seeded at $2x10^5$ cells in 1.5 mL Lebovitz media (phenol red free media) on poly-L-lysine coated 16 mm coverslips in a 12-well plate or 35 mm glass bottom culture dishes and left for 24 h at 37ºC with 5% CO_2. Parent dye (0.05% v/v DMSO in PBS) or octa-arginine conjugate (in aqueous PBS alone) were added to the cells (to achieve a final concentration of 40 µM) and left to incubate for various time intervals. To assess the mode of uptake, cells were prepared as mentioned above and incubated with the complex at 4ºC. Cells were washed with PBS (supplemented with 1.1 mM $MgCl_2$ and 0.9 mM $CaCl_2$) and imaged immediately, using a Zeiss LSM510 Meta Confocal microscope with a heated stage at 37°C. The cells were excited at 488 nm using an argon ion laser and emission was collected using a long pass 650 nm filter. For real-time imaging, 70 µM dye was added and cells were imaged immediately using Time Series mode to capture images every 10 min over a 120 min period.

Cytotoxicity Studies

Cells were seeded in 96-well plates (Nunc F Tissue culture treated plates (Thermofisher)) at $1x10^4$ for CHO cells and $2x10^4$ for SP2 cells in 100 µL media for 24 h at 37ºC with 5% CO_2. The dye complexes or vehicle controls were added for 16 hours at 37ºC with 5 % CO_2. Final dye concentrations were 200, 150, 100, 40, 10, 1 and 0.1 µM. The Alamar blue assay was used to measure cell viability by the addition of 10 µL resazurin reagent and cells were incubated for 7 h at 37ºC in the dark. Absorbance was measured

using a Tecan 96-well plate reader at 570 nm and 600 nm (corrected for background subtraction).

Phototoxicity studies

CHO cells were prepared as described above. Dyes (70 μM) in media were pre-loaded into cells for 24 h. The cells were transferred to a 37°C heated stage and imaged using a Zeiss LSM510 Confocal Microscope. DRAQ7 (Biostatus, UK), which stains the nucleus of dead cells, was added to the culture dish (final concentration 3 μM). DRAQ7 was excited using a 633 nm HeNe laser, osmium and ruthenium were excited at 488 nm (2% transmission) and 458 nm (6 % transmission), respectively using an argon laser. Emission was collected using the long pass 650 nm filter set for DRAQ7 and osmium, and long pass 615 nm filter for ruthenium. An initial image was taken at t=0 to show the loading of the osmium or ruthenium and that the cells were viable. The light was set to 8.5 V and cells were left exposed for 3 h, after which time any uptake of DRAQ7 was recorded.

High Throughput (HTP) Uptake Studies

CHO cells were seeded at 2 x 10^4 cells per well in a 96-well plate, and incubated overnight at 37°C with 5% CO_2. Nuclei were stained using *Hoechst 33342* (Thermofisher scientific) (2 μg/mL) added 20 minutes before measurements. The media was removed and cells washed once with PBS (supplemented with 1.1 mM $MgCl_2$ and 0.9 mM $CaCl_2$). Osmium and ruthenium peptide conjugates (60 μM) were then added to each well (final volume 100 μl). The dye uptake rate was measured by reading five random fields of view per well, using an Insight Cell Analyzer, GE with a 20x objective lens.

Fluorescent lifetime imaging microscopy (FLIM)

CHO cells were seeded on sterile 35 mm glass bottom culture dish and were incubated with 70 μM of each dye for 24 h. Cells were washed with PBS (supplemented with 1.1 mM $MgCl_2$ and 0.9 mM $CaCl_2$) and fixed using 3.8% parafamaldehyde in the dark for 10 min, then washed again. FLIM images were acquired using Microtime 200, PicoQuant attached to a Zeiss LSM510 confocal microscope using 63x oil immersion objective. Each sample FLIM image was acquired for 30 min with 256 x 256 resolution. 405 nm laser was used to excite the sample and emission collected using a long pass 530 nm filter for both osmium and ruthenium. Data was analysed using PicoQuant Symphotime software.

Raman Spectroscopy and Mapping

CHO cells were seeded in 35 mm glass bottom culture dishes and loaded with dye (70 μM) as described above. Raman spectra within different regions of live CHO cells incubated with each dye were collected with a 488 nm laser on a Horiba Jobin-Yvon Labram HR instrument, using a 50 X objective and a 300 μm hole. An exposure time of 10 seconds per spectrum was used and 5 spectra were averaged for each location.

Results and discussion

Synthesis

The structures of the polyarginine conjugated metal complexes described in this report are shown in Scheme 1. $[Ru(bpy)_2(pic)]^{2+}$ and related analogues were synthesized and purified according to protocols reported previously.[39,14] In the case of novel $[Os(bpy)_2(pic)]^{2+}$ ^{1}H NMR, elemental analysis, HPLC and high resolution mass spectrometry were used to confirm the structure and purity of the metal complex. Conjugation of the osmium transition metal complex to the peptide was performed using HATU/DIPEA coupling techniques. Purification of the osmium-peptide was performed by recrystallisation in ethanol:H_2O (1:1 v/v) to give an average yield (44%). HPLC and ^{1}H NMR analysis confirmed the purity of the dye-peptide conjugate. MALDI-ToF analysis confirmed the presence of the osmium-peptide conjugate by exhibiting a molecular ion peak of 2209 m/z, corresponding to the anticipated molecular weight of the conjugated complex. The analogous ruthenium-peptide conjugate was synthesized *via* Merrifield's solid phase peptide synthesis, according to the Fmoc/t-Bu strategy and was previously reported by Neugebauer *et al*.[39]

Photophysics

Table 1 summarises the optical and photophysical properties of the ruthenium and osmium peptide conjugates and their parent complexes. The parent ruthenium complex has been studied in detail by us and others,[37,40,41], whereas the osmium analogue as not been reported to date. As described previously for the ruthenium complex, there was no significant change evident in the optical properties of the osmium complexes upon peptide conjugation.[39] The electronic absorbance and emission spectra of $[Os(bpy)_2(pic)]^{2+}$ and of $[Os(bpy)_2(pic\text{-}arg_8)]^{10+}$ are shown in supplemental material along with, for comparison, the spectra of their ruthenium analogues. $[Os(bpy)_2(pic)]^{2+}$ and its peptide conjugate exhibited a broad visible absorbance extending from approximately 400 to 680 nm. Two visible absorbance maxima were observed at approximately 490 nm and a weaker absorbance 660 nm both attributed to osmium (dπ) to bpy (π*) transitions. The lower energy optical transition is attributed to a singlet to triplet absorbance and is not observed for the ruthenium complexes due to stronger spin orbit coupling from the greater mass of the osmium

nuclei.[42,17] $[Os(bpy)_2(pic)]^{2+}$ exhibits an emission maximum at λ_{max} 726 nm with a quantum yield of 0.0022 when excited into its MLCT absorbance. Although it has a relatively low quantum yield, its large Stoke shift allows the osmium complex to be used at relatively high concentrations without self-quenching. The osmium complex has a relatively short luminescent lifetime of 33 ns which renders its emission O_2 independent. This is in contrast with the ruthenium analogue which exhibits a lifetime of between 540 ns and 872 ns depending on the dissolved oxygen concentration within the solution. Nonetheless, a lifetime of 33 ns can be easily resolved from the autofluorescent lifetimes observed from cells and tissues and is long enough to be useful in luminescence anisotropy studies, e.g. for microviscosity or protein binding within cells.[43,18]

Another key advantage of the osmium polypyridyl complexes over their ruthenium analogues is their remarkable photostability and the associated weak temperature dependence of their emission properties. As shown in Table 1 unlike its ruthenium analogue, the lifetime of the osmium complex does not vary between room temperature and 37°C used to image cells. To compare the photostability of the osmium and ruthenium analogues in the context of their application in cellular imaging, each parent complex was assessed in PBS buffer by irradiating 70 μM solutions of $[Os(bpy)_2(pic)]^{2+}$ or $[Ru(bpy)_2(pic)]^{2+}$ with 488 nm or 458 nm laser at 30% laser power (i.e. the conditions which are used to induce probe bleaching in fluorescence recovery after photobleaching experiments) for two consecutive 10 minute intervals. The emission intensities of the irradiated solution was imaged immediately after each interval at a laser power of 1% to assess any changes in emission intensity (in FRAP format). Interestingly, it was found that $[Os(bpy)_2(pic)]^{2+}$ is significantly more stable than $[Ru(bpy)_2(pic)]^{2+}$. No photo-bleaching was detected for the osmium complex even over extended periods of high intensity irradiation; conditions under which the ruthenium analogue decomposed (Supplemental Figure S9). The stability of the osmium complex suggests their potential as cellular imaging agents, particularly for applications involving dynamic studies requiring long dye exposure times, for example in fixed cells and tissues.

Cell Uptake Studies

Uptake of $[Os(bpy)_2(pic)]^{2+}$, $[Ru(bpy)_2(pic)]^{2+}$ and their octa-arginine conjugates by CHO cells and SP2 myeloma cells were compared. Figure 1 shows confocal luminescence images of live SP2 cells collected following 2 h incubation with 70 μM (A) $[Ru(bpy)_2(pic\text{-}arg_8)]^{10+}$ and (B) $[Os(bpy)_2(pic\text{-}arg_8)]^{10+}$. Neither of the unconjugated parent complexes permeated the cell on incubation, although permeation could be induced by including detergent (Triton) or 0.5% v/v DMSO in the media. In contrast, the octa-arginine conjugates were transported rapidly across the cell membrane without permeabilization. For the $[Os(bpy)_2(pic\text{-}arg_8)]^{10+}$, consistent with the behaviour of the ruthenium analogue, this process was found to be activate

Incubation of $[Os(bpy)_2(pic\text{-}arg_8)]^{10+}$ with either cell line at 4°C inhibited uptake. Real-time imaging showed that $[Os(bpy)_2(pic\text{-}arg_8)]^{10+}$ crosses the cell membrane and distributes in the cell cytoplasm within a matter of minutes (Supplementary videos 1-3).

Compound	λ_{abs} (nm)	λ_{em} (nm)	ϕ (quantum yeild)	τ/ns
$[Os(bpy)_2(pic)]^{2+}$	484	720	0.0022± 0.0007¶	33 ± 0.1 [a] 31 ± 1.9 [b] 33 ± 1.1 [c]
	488*	726*	0.01*	57* ± 0.4
$[Os(bpy)_2(pic\text{-}arg_8)]^{10+}$	486	726	0.0025 ± 0.0008¶	31 ± 0.2 [a] 29 ± 2.05 [b] 33 ± 2.47 [c]
$[Ru(bpy)_2(pic)]^{2+}$	458	608	0.067	540 [a] 624 [b] 872 ± 4 [c ξ]
$[Ru(bpy)_2(pic\text{-}arg_8)]^{10+}$ ξ	470	610	0.06	478 [a] 514 ± 4.9 [b] 775 ± 4 [c]

Table 1. Spectroscopic and photophysical data for $[Os(bpy)_2(pic)]^{10+}$ and $[Ru(bpy)_2(pic)]^{10+}$ and their peptide conjugates in various media. ξFrom Neugebauer *et al.*[39]

* In degassed acetonitrile at room temperature. ¶ Quantum yields were measured in aerated PBS solution. φ values were calculated using $[Ru(bpy_3)]^{2+}$ = 0.028 as standard.[44,19]

[a] measured at room temperature (approx. 18°C), [b] 37°C, [c] in de-aerated PBS solution by purging with nitrogen for 20 min.

Over the first 2 minutes the dye concentrates in the cytoplasm, after which it proceeds to distribute throughout the different intra-cellular components. These results are similar to the reported findings for the $[Ru(bpy)_2(pic\text{-}arg_8)]^{10+}$ uptake by SP2 cells where the conjugate rapidly traversed the membrane but did not penetrate the nuclear envelope membrane.[39] Interestingly, $[Os(bpy)_2(pic\text{-}arg_8)]^{10+}$ appeared to enter the nucleoli of both SP2 cells and CHO cells during live uptake studies under imaging conditions, (Supplementary Figure 5). However, nucleoli uptake did not occur when the conjugate was incubated with cells in the dark for 2 h for either cell line. This observation suggests that nuclear uptake for this complex is photo or thermally activated. Interestingly, analogous behaviour was not noted for the ruthenium peptide.[45,20] Co-localization studies involving $[Os(bpy)_2(pic\text{-}arg_8)]^{10+}$ in CHO were carried out using MitoTracker Deep Red and LysoTracker Green which showed preferential localization in the mitochondria and

lysosome respectively. These studies indicated that $[Os(bpy)_2(pic\text{-}arg_8)]^{10+}$ localized in some, but not all, mitochondria and that it also penetrates the lysosomes (Supplementary Figure S7 (iv)). This is consistent with conjugation to the octa-arginine peptide which is regarded as a general cytoplasmic targeting carrier. Figure S7 (iv) C and D show the results from high throughput (HTP) uptake studies. HTP was carried out here because of the evident effect of continuous scanning on the localization of the $[Os(bpy)_2(pic\text{-}arg_8)]^{10+}$ within cells. HTP is a useful means of screening uptake as it monitors large numbers of cells ensuring statistical significance of the results and reduces imaging time at single cells, thus avoiding issues such local thermal or light induced effects which may inadvertently promote uptake. The $[Os(bpy)_2(pic\text{-}arg_8)]^{10+}$ and $[Ru(bpy)_2(pic\text{-}arg_8)]^{10+}$ were both studied by this method, whereby 70 μM of the complex conjugate was incubated with CHO cells and the intensity of emission from the cells measured across a 2 h period at 37°C. This data showed that although initial uptake is rapid the probe continues to accumulate within the cells over 2 h after which time uptake plateaus. Under HTP imaging, the osmium complex showed fewer tendencies to reach the nucleoli, indicating that its entry to this organelle was thermally or photochemically promoted.

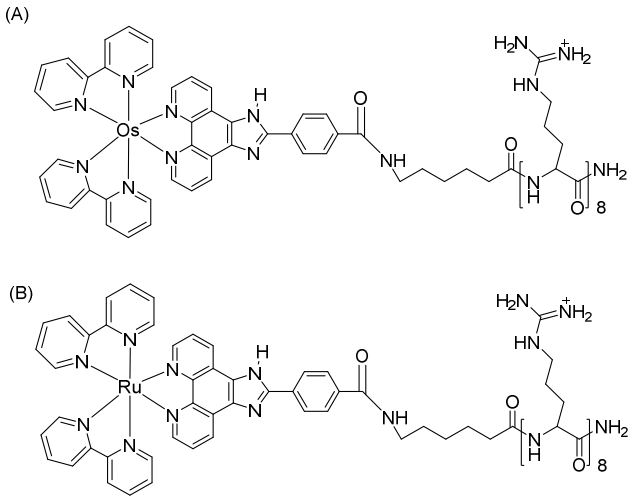

Scheme 1 Structures of (A) $[Os(bpy)_2(pic\text{-}arg_8)]^{10+}$ and (B) $[Ru(bpy)_2(pic\text{-}arg_8)]^{10+}$.

FLIM and Oxygen Sensitivity Studies

A key advantage of using metal polypyridyl complexes, such as osmium or ruthenium, in cell imaging is their relatively long emission lifetimes which give rise to environmentally sensitive emission characteristics which can be monitored by their lifetime imaging distribution.

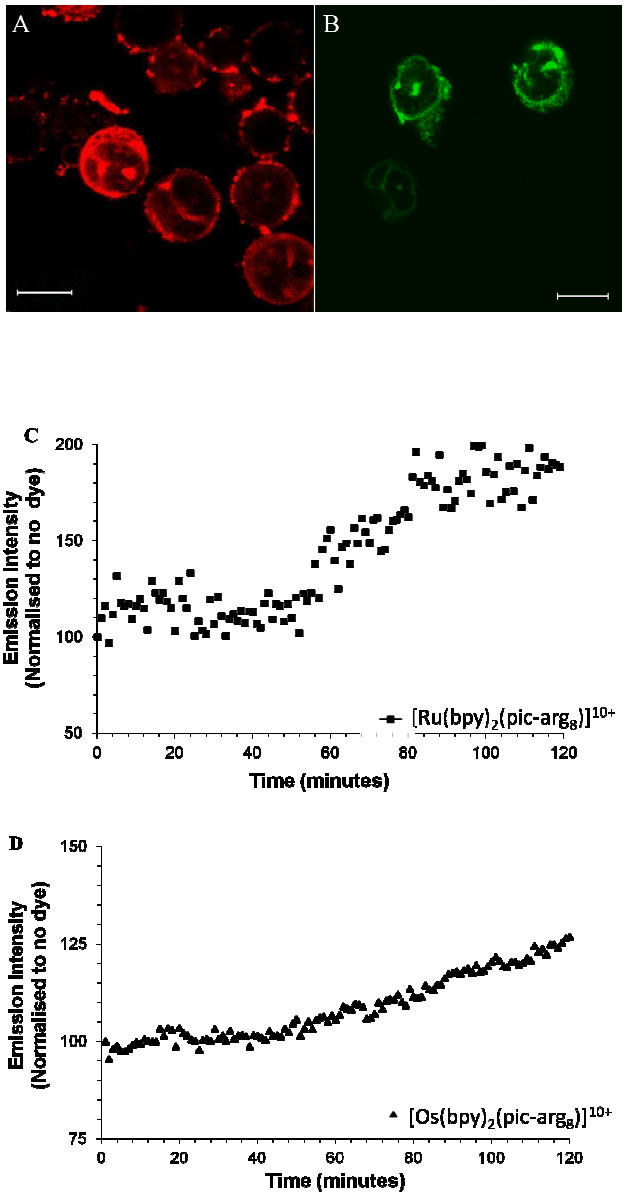

Figure 1 Cellular uptake of (A) $[Ru(bpy)_2(pic\text{-}arg_8)]^{10+}$ and (B) $[Os(bpy)_2(pic\text{-}arg_8)]^{10+}$ by live SP2 cells after 2 h incubation at 37°C showing nucleoli penetration (z = 2, scale bar = 10 μM). HTP uptake studies of (C) $[Ru(bpy)_2(pic\text{-}arg_8)]^{10+}$ and (D) $[Os(bpy)_2(pic\text{-}arg_8)]^{10+}$ in CHO cells.

An important benefit of lifetime imaging over intensity based methods is that the emission lifetime is independent of the concentration of the probe. $[Ru(bpy)_2(pic)]^{2+}$ exhibits a lifetime of 540 ns in aerated aqueous solution and strong O_2 sensitivity; wherein the lifetime increases to 872 ns in de-aerated media. This response to the presence of oxygen permits the concentration of oxygen to be mapped within the cell using FLIM.[46,22] Conversely, $[Os(bpy)_2(pic\text{-}arg_8)]^{10+}$ exhibits a lifetime of 33 ns in acetonitrile, which we observed to be independent of O_2 concentration (Supplementary Figure 3). Figure 2 shows the lifetime imaging of (A) $[Os(bpy)_2(pic\text{-}arg_8)]^{10+}$ and (B) $[Ru(bpy)_2(pic\text{-}$

$arg_8)]^{10+}$ in SP2 cells The average lifetime of osmium within the cell was found to be 20 ± 0.9 ns.

A lifetime of 18.8 ± 0.6 ns was observed at the cell membrane and 14.5 ± 0.5 ns in the cytoplasm indicated by the lifetime components in the false-colour distribution image. Similar results were observed from FLIM imaging of $[Os(bpy)_2(pic\text{-}arg_8)]^{10+}$ in CHO cells (Supplementary Figure 8). Here interestingly, the average lifetimes were found to be 13 ± 1.5 ns in the membrane and 11.6 ± 0.4 ns in the cytoplasm.

Although the osmium luminescence is not sensitive to oxygen, its emission lifetime does appear to change in response to environment as demonstrated by the variations in the cytoplasmic lifetimes between the two cell lines. Similar variation in average luminescent lifetime with cell type was observed for $[Ru(bpy)_2(pic\text{-}arg_8)]^{10+}$ which exhibited an average lifetime of 453 ± 25 ns in the cell membrane and 540 ± 12 ns in the cytoplasm of SP2 mouse myeloma cells.[39] As the osmium luminescent lifetime is not affected by oxygen concentration it is likely that local viscosity at the membrane may be affecting the osmium lifetime in this region of cell.[43] The increase in $[Os(bpy)_2(pic\text{-}arg_8)]^{10+}$ lifetimes seen in the membrane compared to the cytoplasmic region suggests that it could be a result of tight lipid packing in the plasma membrane. [47] Under similar experimental conditions, a decrease in $[Ru(bpy)_2(pic\text{-}arg_8)]^{10+}$ lifetime was demonstrated in the membrane compared to the cytoplasm by Neugebauer *et al.* which was attributed to the greater solubility of O_2 in membrane regions.[39]

Resonance Raman Spectroscopy

The broad visible absorbance and large Stokes shift of these complexes make them readily amenable to study by resonance Raman microscopy. In resonance Raman spectroscopy the Raman excitation wavelength is resonant with an optical transition and Franck Condon vibrational modes associated with the chromophores and exhibit Raman scattering enhancements of typically 2 to 6 orders of magnitude. Transitions which are strongly allowed exhibit best enhancements and thus resonance Raman spectroscopy has been exploited widely to elucidate the origin of optical transitions in transition metal complexes.[47,48]

Resonance Raman microscopy is a very useful way of selectively monitoring the structure of a probe against a complex background such as that of cells or tissues. Because of their large Stokes shifts metal complexes are particularly attractive in this regard as both luminescence and resonance Raman can be exciting under the same wavelength without mutual interference. The resonance Raman spectra of $[Os(bpy)_2(pic)]^{2+}$ and its peptide conjugate were collected from a 70 μM PBS solution exciting at 488nm and the resulting spectra are shown in Figure 3. The spectra were normalised to the 1317 cm^{-1} vibration as this bipyridine ligand mode is well isolated from the pic ligand modes and shows little dependence on the environment.[46,39]

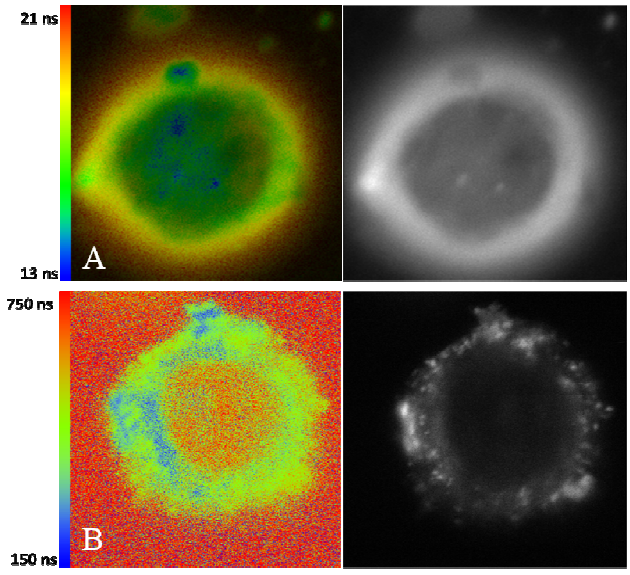

Figure 2. Fluorescent lifetime image of (A) $[Os(bpy)_2(pic\text{-}arg_8)]^{10+}$ and (B) $[Ru(bpy)_2(pic\text{-}arg_8)]^{10+}$ in live SP2 cell. SP2 cells were incubated with 70 μM $[Os(bpy)_2(pic\text{-}arg_8)]^{10+}$ for 24 h and 350 μM $[Ru(bpy)_2(pic\text{-}arg_8)]^{10+}$ for 15 min. Both complexes imaged using the 405 nm excitation laser line and emission collected using long pass 530 nm filter (zoom = 10x).

Other signature vibrational modes for the bipyridine ligand are observed at 1603, 1552, 1482, 1269, 1173, 1024 and 670 cm^{-1}. Interestingly, following excitation into its MLCT transition at 488 nm, the osmium complex exhibited features associated with the pic ligand moieties which were of comparable intensity to bpy ligand modes at 1625, 1556, 1506 cm^{-1}, 1458, 1422, 1248, 1198 and 829cm^{-1}. By comparison, the resonance Raman spectrum of the ruthenium analogue (excited into the MLCT transition at 458 or 488 nm) exhibited few vibrational bands that were characteristic of the pic ligand and those that were evident were weak when compared to the bpy vibrational modes. In the ruthenium complex the presence of pic modes in the resonance Raman spectra was attributed to post resonance with a pic π- π* transition centred around 400 nm. The intensity and complexity of the Raman signature from the pic ligand in the resonance Raman spectrum of the osmium complex suggests resonance with both a Os(dπ) to pic π* MLCT transitions and Os(dπ) to bpy π* transition at this excitation wavelength as the energy of the π-π* transition of the ligand is not expected to change significantly between ruthenium and osmium coordination.[49,50,51] As shown in Figure 3, the resonance Raman spectra of the osmium complex and its peptide conjugate are indistinguishable which is expected since the peptide does not contribute to the visible optical transitions.

Given the high quality of the resonance Raman spectra of $[Os(bpy)_2(pic\text{-}arg_8)]^{10+}$ at micro-molar concentrations in

solution we were interested to see if we could study the distribution of the peptide probe in live cells. This was assessed in CHO cells following their incubation for 24 h with 70μM of $[Os(bpy)_2(pic\text{-}arg_8)]^{10+}$.

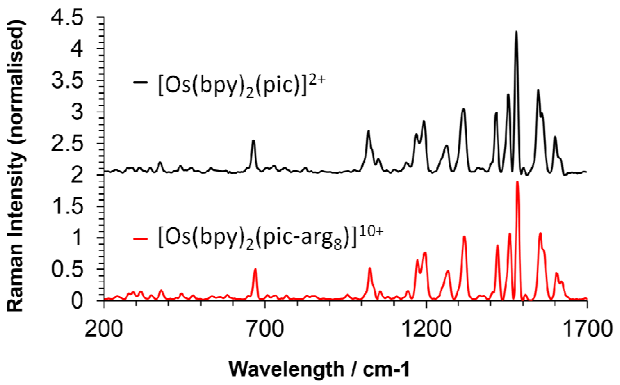

Figure 3 Raman spectra of $[Os(bpy)_2(pic)]^{2+}$ and its octa-arg conjugate each at 70 μM in PBS. Excitation wavelength was 488 nm and spectra were aquired for 64 s. (n=3) Spectra are normalised to the bipyrdine vibrational mode at 1317 cm^{-1})

The resonance Raman spectra were recorded from the different cellular regions; membrane, cytoplasm and nuclear regions and compared with the resonance Raman from the contacting solution and of the osmium conjugate in PBS solution (Figure 4). High quality Resonance Raman spectra were obtained from the probe within live cells exciting at 488 nm with an acquisition time of 64 s. Although the spectra are normalised, it is evident from the poorer signal to noise ratio and the relative intensity of broad band centred around 900 cm^{-1} arising from the phosphate buffer, which is not resonantly enhanced, that the $[Os(bpy)_2(pic\text{-}arg_8)]^{10+}$ is present at relatively low concentrations outside the cell; indicating that it has selectively accumulated within the cell. Interestingly, there are some notable changes in the relative intensity of key bands for the conjugate inside the cell compared to in free media. The pic based mode at 1458 cm^{-1} exhibits a nearly 3-fold intensity increase relative to the bipyridyl reference band at 1482 cm^{-1} mode in the cell compared to the complex in solution. The aromatic ring stretch coupled CH mode at 1552 cm^{-1} exhibits a shoulder at 1559 cm^{-1} in PBS, which disappears when the complex is within the cell, and instead a shoulder at 1549 cm^{-1} appears.[52] The origin of this change within the cellular environment is not clear but may arise from alterations to the pH of the environment affecting the imidazole nitrogen on the osmium complex, Such effects were noted for the ruthenium complex but appear to be even stronger for the osmium reported here.[46]

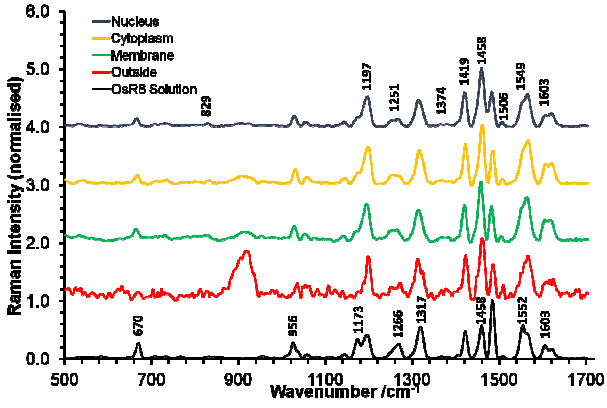

Figure 4 Raman mapping and spectra of $[Os(bpy)_2(pic\text{-}arg_8)]^{10+}$ obtained using a 488 nm excitation wavelength. Results are representative of three separate experiments. CHO cells were incubated with 70 μM $[Os(bpy)_2(pic\text{-}arg_8)]^{10+}$ for 24 h and washed with PBS buffer (pH 7.4). Data was normalised to the peak vibration at 1458 cm^{-1}

Both Osmium and Ruthenium Bipyridyl Complexes Exhibit Low Cytotoxicity.

An important consideration, if osmium(II) polypyridyl complexes are to find application in cell imaging, is their cytotoxicity. The viability of mammalian cells treated with $[Os(bpy)_2(pic)]^{2+}$, $[Os(bpy)_2(pic\text{-}arg_8)]^{10+}$, $[Ru(bpy)_2(pic)]^{2+}$ and $[Ru(bpy)_2(pic\text{-}arg_8)]^{10+}$ was assessed by incubating each complex overnight with CHO (Figure 5A) and separately with SP2 myeloma cells (Figure 5B) at 37°C with 5% CO_2. The Alamar blue viability assay was used to assess and quantify the extent of cell death. This assay measures the reduction of resazurin to fluorescent resorufin and dyhydroresorufin by viable cells. Encouragingly, neither the osmium nor ruthenium parent complexes (introduced into the cells from solution containing DMSO (0.1% v/v) solvent to permeablize the cells) were cytotoxic even upto extended >24 h incubation periods and at concentrations up to 200 μM; considerably more than required for imaging. Similarly, their octa-arginine conjugates induced little toxicity towards CHO cells (Figure 5A) under imaging conditions, however $[Os(bpy)_2(pic\text{-}arg_8)]^{10+}$ did exhibit cytotoxicity toward SP2 cells at concentrations exceeding 100 μM (Figure 5B). We have observed previously for an iridium complex that octa-arginine increased its cytotoxicity and in addition modest cytotoxicity of polyarginines toward mammalian cells has been noted previously by others.[53,54,55] Why this cytotoxicity is seen selectively at SP2 cells and not CHOs in the present study is unclear.

The cytotoxicity assay shown in Figure 5 was carried out following incubation of complex or conjugate with the cells in the dark. To test for phototoxicity, test cells which had been pre-incubated with the complexes or conjugates in the dark were irradiated with a continuous white light source

(0.0049 J/s) for 2 h. Toxicity was assessed by determining the amount of the viability dye, DRAQ7 (which only enters compromised cells), that had accumulated within the cell nuclei following irradiation. Remarkably, no DRAQ7 was found to have entered the cells following over 2 h constant illumination of the samples in the presence of complex/conjugate. This is an important result and suggests that both the osmium and ruthenium bipyridyl complexes and particularly their arginine conjugates, are non-photocytotoxic under the conditions used for imaging.

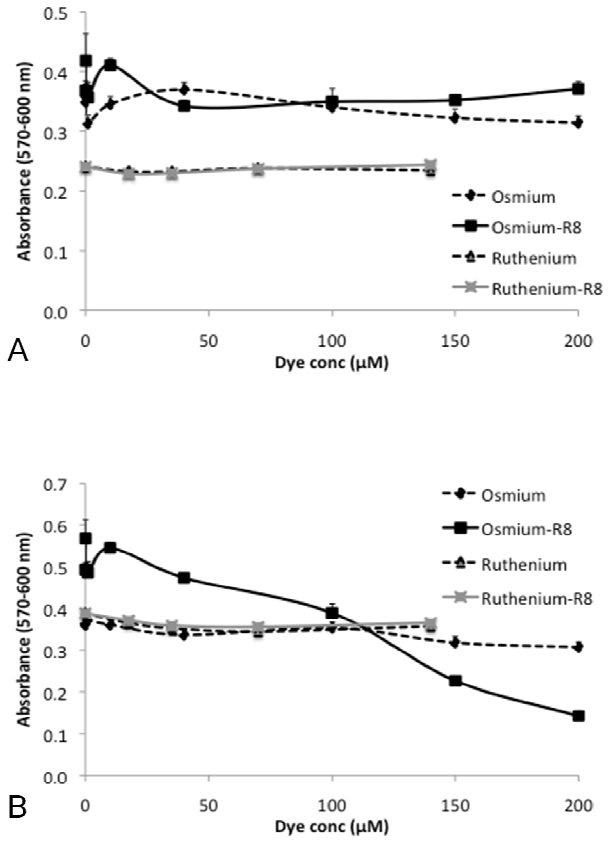

Figure 5 Cell viability of (A) CHO and (B) SP2 cells after overnight exposure to the metal complexes. Live cells were treated with $[Os(bpy)_2(pic)]^{2+}$ (Osmium), $[Os(bpy)_2(pic\text{-}arg_8)]^{10+}$(Osmium-R8), $[Ru(bpy)_2(pic)]^{2+}$ (Ruthenium) and $[Ru(bpy)_2(pic\text{-}arg_8)]^{10+}$ (Ruthenium-R8) for 16 h followed by addition of resazurin reagent for another 6 h. Absorbance was read at 570 nm with background at 600 nm subtracted, n=3, data have been offset for clarity.

Conclusions

We present the first application of an osmium(II) polypyridyl complex to live cell imaging. The novel complex $[Os(bpy)_2(pic)]^{2+}$ and its octaarginine conjugate $[Os(bpy)_2(pic\text{-}arg_8)]^{10+}$ were prepared and their photophysical properties, cell uptake and cytotoxicity were compared with their ruthenium analogues. The osmium complexes exhibited red emission centred around 726 nm, which is usefully situated inside the biological window and out of the range of cellular autofluorescence. The luminescent lifetime of $[Os(bpy)_2(pic)]^{2+}$ was significantly shorter than that of its ruthenium analogue, at 33 ns in acetonitrile, which was unaffected by peptide conjugation. Neither parent nor peptide conjugate were oxygen responsive. Their luminescent lifetime were unaffected by deaeration. The osmium complex, unlike its ruthenium analogue also showed no change in luminescence lifetime between room temperature (18°C) and 37°C used for imaging.

$[Os(bpy)_2(pic)]^{2+}$ was cell impermeable without the use of DMSO or detergent. Following octa-arginine conjugation however, $[Os(bpy)_2(pic\text{-}arg_8)]^{10+}$ was rapidly internalised and distributed around the cell cytoplasm by an activated membrane transport process. High throughput screening showed that uptake was very similar for both ruthenium and osmium analogues. Although nuclear excluding, the $[Os(bpy)_2(pic\text{-}arg_8)]^{10+}$ penetrated the nucleus in a process that was light dependent. Fluorescence lifetime imaging studies showed the lifetime of $[Os(bpy)_2(pic\text{-}arg_8)]^{10+}$ was reduced in the cell compared to solution and that it was also significantly different in the cell membrane of CHO cells (11.6 ± 0.4 ns) and SP2 cells (18.8 ± 0.6 ns). As $[Os(bpy)_2(pic\text{-}arg_8)]^{10+}$ showed no oxygen sensitivity, these changes were attributed to the different membrane structures between the two cell lines.

Intense high quality resonance Raman spectra were obtained from $[Os(bpy)_2(pic\text{-}arg_8)]^{10+}$ within cells at concentrations suitable for luminescence imaging. Somewhat surprisingly, neither $[Os(bpy)_2(pic)]^{2+}$ nor $[Os(bpy)_2(pic\text{-}arg_8)]^{10+}$ were found to be cytotoxic towards CHO or SP2 cells at concentrations appropriate to imaging (50 to 100 μmol) over 24 or 48 h exposure. The osmium complexes showed remarkable photostability in cell media and under conditions conventionally used to generate luminescent recovery after photobleaching, unlike their ruthenium analogues the osmium complexes did not bleach within the cells. This along with their red emission may make them suitable for cell imaging particularly in applications requiring long irradiation times.

Overall, this study shows that osmium(II) polypyridyl complexes may offer a useful addition to the growing repertoire of metal based imaging probes, particularly in applications involving long-time scale dynamic experiments which place significant demands on the stability of the probe.

ASSOCIATED CONTENT

Supporting Information.
Spectra of parent complexes
Lifetime decays
Oxygen Studies
FLIM

Videos of $[Os(bpy)2(pic\text{-}arg8)]^{10+}$uptake
Cell Viability Studies

"This material is available free of charge via the Internet at http://pubs.acs.org." For instructions on what should be included in the Supporting Information as well as how to prepare this material for publication, refer to the journal's Instructions for Authors.

ACKNOWLEDGMENTS

This material is based upon work supported by the Science Foundation Ireland Grant No. 10/IN.1/B3025 and 12/TIDA/B2382 by the Irish Programme for Research in Third Level Institutions, Cycle 4, Ireland's EU Structural Funds Programmes 2007 - 2013.
The authors gratefully acknowledge the Irish Government's Programme for Research in Third Level Institutions, Cycle 4, Ireland's EU Structural Funds Programmes 2007–2013 for support of the National Biophotonics and Imaging Platform, Ireland. The CAN project (Project No. 85) has been part-funded by the European Regional Development Fund through the Ireland Wales Programme 2007-13.

ABBREVIATIONS

FLIM Fluorescence Lifetime Imaging Microscopy

REFERENCES

[1] M Peana, V.M. Nurchi, J.I. Lachowicz, G. Crisponi, M.A. Zoroddu, Coord. Chem Rev., 284, 329-350

[2] Q. Zhao, C.H. Huang, FY. Li, Chem Soc. Rev., 2011, 40, 2508.

[3] V. Fernandez-Moreira, F.L. Thorp-Greenwood, M.P. Coogan, *Chem. Commun.* **2010**, *46*, 186.

[4] K. K.-W. Lo, P.-K. Lee and J. S.-Y. Lau, Organometallics, **2008**, 27, 2998.

[5] E. Baggaley, J.A. Weinstein, JAG. Williams, Coord. Chem. Rev.2012, 256, 1762.

[6] A.K. Pal, N. Zaccheroni, S Campagna, G.S. Hanan, Chem. Comm. 2014, 50, 6846.

[7] S. Rau, S.Z. Zheng, Curr. Top. Med. Chem., 2012, 12, 197.

[8] A.Martin, A. Byrne, C. S. Burke, R. J. Forster, T.E. Keyes, J.Am. Chem. Soc., 2014, 136, 15300-9.

[9] A Wragg, M.R.Gill D Turton, H Adams, TM Roseveare, C Smythe, XD Su, JA Thomas, Chem. A Europ . J, 2014, 20, 14004-14011

[10] J. Kuil, P. Steunenberg, PTK. Chin, J. Oldenburg, K. Jalink, A.H. Velders, F.W.B. van Leeuwen, ChemBio-Chem, 2011, 12, 1896.

[11] M. Dickerson, Y Sun, B Howerton, B, EC. Glazer, Inorg Chem, 2014, 53, 10370-10377

[12] Q. Shao, B.G. Xing, Chem. Comm, 2012, 48, 1793.

[13] C.A. Puckett and J. K. Barton, Bioorg. Med. Chem. 2010, 18, 3564.

[14] O. Mazuryk, Magiera, K Rys, B Suzenet, F Kieda,; Brindell, M, J Biol Inorg Chem, 2014, 19,1305

[15] C Sanchez-Cano, MJ Hannon, Dalton Trans., 2009, 10765-10773.

[16] A. C. Komor , C. J. Schneider , A. G. Weidmann , J. K. Barton J. Am. Chem. Soc. 2012, 134 19223

[17] F. Pierard, A. Kirsch-De Mesmaeker, Inorg. Chem. Comm., **2006**, 9, 111.

[18] Q. Zhao, M. Yu, L. Shi, S. Liu, C. Li, C.; Shi, Z. Zhou, Z.; C. Huang, F. Li, *Organometallics* **2010**, *29*, 1085.

[19] L.; Xiong, Q.; Zhao, H.; Chen, Y.; Wu, Z.; Dong, Z.; Zhou, F.Li, *Inorg. Chem.* **2010**, *49*, 6402-6408.

[20] C.; Dolan, R.D. Moriarty, E. Lestini, M. Devocelle, R.J. Forster, T.E. Keyes, *J. Inorg. Biochem.* **2013**, *119*, 65-74.

[21] J.K. Barton, E. D. Olmon and P. A. Sontz, Coord. Chem. Rev.2011, 255, 619

[22] Y. J.; Liu, C. H.; Zeng, H. L.; Huang, , L. X.; He F. H Wu,. **2010**, *45*, 564-571.

[23] M.R. Gill, J.A. Thomas, *Chem. Soc. Rev.* **2012**, *41*, 3179.
[24] B. Pena, R. Barhoumi, RC. Burghardt, C. Turro, KR. Dunbar, J. Am. Chem. Soc, 2014, 136, 7861-7864

[25] S. H. van Rijt, A. Mukherjee, A. M. Pizarro, P. J. Sadler, *J. Med. Chem.* **2010**, *53*, 840-849.

[26] S. H. van Rijt, I. Romero-Canelón, Y. Fu, S. D. Shnyder, P. J. Sadler, *Metallomics* **2014**, *6*, 1014-1022.

[27] S. H.; van Rijt, Kostrhunova, H.; Brabec, V.; Sadler, P. J. *Bioconjugate Chem.* **2011**, *22*, 218-226.

[28] W. F.; Schmid, R. O.; John, V. B.; Arion, M. A.; Jakupec, B. K. Keppler, *Organometallics* **2007***, 26*, 6643-6652.

[29] H Kostrhunova,. J. Florian, O.; Novakova, A. F. A.; Peacock, P. J.; Sadler, V. *J.* Brabec, *Med. Chem. 2008, 51, 3635–3643* **2008***, 51*, 3635-3643.

[30] B. Durham, J.L. Walsh, C.L. Carter, T.J. Meyer, *Inorg. Chem*., **1980**, 19, 860.

[31] R.S. Lumpkin, E.M. Kober, L.A. Worl, Z. Murtaza, T.J. Meyer, *J.Phys. Chem*. **1990**, 94 239

[32] T.E. Keyes, D. Leane, R.J. Forster, C.G. Coates, J.J. McGarvey, J.G. Vos, *Inorg. Chem*., **2002**, 41, 5721,.

[33] D. Leane, T.E. Keyes, Inorg. Chim. Acta, 2006, 40, 1627

[34] T.E. Keyes, C.E M. O'Connor, U. O'Dwyer, C. G. Coates, P Callaghan, J. J. McGarvey, J. G. Vos, J. Phys. Chem. A, 1999, 103, 8915.

[35] Z. J. Fuller.; W. D. Bare.; K. A. Kneas.; W.-Y. Xu.; J. N. Demas.; B. A. DeGraff. *Anal. Chem*. **2003**, 75, 2670-2677

[36] Juris, F.; Balzani, V.; Barigelletti, Campagna, S.; Belser, P.; von Zelewsky, A.Coord. Chem. Rev, 1988,

82, 85.

[37] G.-Y. Bai, B. Dong, Y.-Y. Lü, K.-Z. Wang, L.-P. Jin, L.-H. Gao, *J. Inorg. Biochem*., **2004**, 98, 2011-2015.

[38] Hoertz et al. J. Am. Chem. Soc. 2006, 128, 8234-8245

[39] Neugebauer, U.; Pellegrin, Y.; Devocelle, M.; Forster, R. J.; Signac, W.; Moran, N.; Keyes, T. E. *Chem. Commun. ,* **2008***, 42*, 5307-5309.

[40] A. Quaranta, F. Lachaud, C. Herrero, R. Guillot, M.-F. Charlot, W. Leibl, A. Aukauloo, Chem. Eur. J., 2007, 13 8201.

[41] Y. Pellegrin, R. J. Forster and T. E. Keyes, Inorg. Chim Acta. 2008, 27, 6, 1690

[42] I. Fujita , H. KobayashiZeitschrift für Physikalische *Chemie*. **1972**, 79, 309–314.

[43] Suhling, K.; French, P. M. W.; Phillips, D. *Photochem. Photobiol. Sci.* **2005***, 4*, 13-22

[44] N. Nakamaru, Bull. *Chem. Soc. Jpn*., **1982**, 55, 2697.

[45] F. R.; Svensson, M.; Matson, M. Li, P. Lincoln, *Biophys. Chem.* **2010***, 149*, 102-106.

[46] U.: Neugebauer, L.; Cosgrave, Y.; Pellegrin, M.; Devocelle, R.J. ; Forster, T.E. Keyes, *Proceedings of SPIE*. **2012**, 8472-84270C.

[47] Stöckl, M. T.; Herrmann, A. *Biochimica et Biophysica Acta (BBA) - Biomembranes* **2010***, 1798*, 1444-1456

[48] Browne, W.R.; McGarvey, J.J. Coord. Chem.Rev. **2007,** 454–473

[49] Pellegrin, Y.; Forster, R.J.; Keyes, T.E Inorg. Chim Acta. **2008**, 361, 2683-2691.

[50] Keyes, T. E.; Forster, R. J.; Jayaweera, P. M.; Coates, C. G.; McGarvey, J. J.; Vos, J. G. Inorg. Chem. **1998**, 37, 5925-5932.

[51] Zhang, X.; Yin, H.; Cooper, J. M.; Haswell, S. J. *Anal Bioanal Chem* **2008***, 390*, 833

[52] P.K Mallick,., G.D., Danzer, D.P. Strommen, J.R., Kincaid, J. Phys. Chem., 1988, 92, 5628. (

[53] Dolan, C.; Moriarty, R.; Lestini, E.; Devocelle, M.; Forster, R.J.; Keyes, T.E. 2013. J. Inorg. Biochem., 119, pp. 65-74.

[54] S.W. Jones, R. Christison, K. Bundell, C. Voyce, S.M.V. Brockbank, P. Newham, M.A. Lindsay, J Pharmacol. 145 (2005) 1093–1102

[55] A. Gross, H. Alborzinia, S. Piantavigna, L. L. Martin, S.Wölfl and N. Metzler-Nolte, Metallomics, 2015,7, 371-384

Table of Contents

The first example of a cell permeable osmium(II) polypyridyl peptide conjugate $[Os(bpy)_2(pic)arg_8]^{10+}$ employed as an contrast agent for live cell imaging is reported.